This is the accepted version of the publication Zhou, Y., Mui, K. W., Wong, L. T., Tsui, P. H., & Chan, W. K., Aerosol generation rates for showerheads, Building Services Engineering Research and Technology (Volume 40 and issue 5) pp. 595-610. Copyright © 2019 (The Author(s)).
DOI: 10.1177/0143624418824839.

Aerosol generation rates for showerheads

Yang Zhou[1], Kwok Wai Mui[2], Ling Tim Wong[3,*], Pak Hei Tsui and Wing Ki Chan

Department of Building Services Engineering,

The Hong Kong Polytechnic University,

Hong Kong, China

[1] yang.zhou@connect.polyu.hk

[2] behorace@polyu.edu.hk

Corresponding Author: L.T. Wong

[3,*] beltw@polyu.edu.hk

Abstract

Aerosolization of water from discharging water appliances provides a transmission medium for Legionnaires' disease. The quantity of aerosolized droplets influences the infection of Legionnaires' disease. This study investigates the aerosol generation rates of four sample showerheads experimentally in a mechanically ventilated test chamber, assisted by computational fluid dynamics (CFD) simulations. The results show that aerosol mass generation rate decreases with the showerhead resistance factor but increases with the water supply pressure, nozzle area ratio, flow rate, spray jet velocity, momentum and force. There is no significant correlation between aerosol mass generation rate and water spray uniformity ($p>0.05$, t-test). Furthermore, the aerosol mass generation rates and aerosol particle generation rates determined for the sample showerheads are in the ranges of 1.42×10^{-5} to 5.52×10^{-5} gs^{-1} and 0.35×10^{6} to 1.35×10^{6} particles s^{-1} respectively.

***Practical applications*:** The proposed expression of aerosol generation rate can be the referenced guidance for future showerhead design to limit the aerosol generation rate.

Keywords

Aerosol generation, showerhead, chamber test, computational fluid dynamics (CFD), Legionnaires' disease (LD)

Nomenclature

A	area
a	acceleration
d	distance
D_s	showerhead diameter
h	height
K_s	showerhead resistance factor
m	aerosol mass
m_0	mass of the water left on the electronic scale after showering
M_s	spray jet momentum
n	number of tracked aerosols
P_s	water supply pressure
p	probability of a specified statistical test of significance
Q_s	water supply flow rate
u	mass flux density
V_s	aerosol volume
v_s	spray jet velocity
ϕ	fraction as defined in an equation
θ_s	spray spread angle

ρ_d, ρ_t	densities of water and saltwater
τ	time period

Subscript

1,2,3	of shower nozzle diameters 1 mm, 2 mm, 3 mm
A	of area
c	of chamber air
d	of distance
f	of faceplate
g	of generation
i	of inflow
max	of maximum
o	of outflow
r	of reading
s	of shower
t	of salt to water
u	of uniformity
w	of wall

Superscript

$\overline{\ }$	of average
$'$	of gradient
$\dot{\ }$	of rate of change with respect to time

Introduction

It has been recognized that aerosols are generated with showerhead discharging, which provide a transmission medium of Leionnaires' disease (LD), a severe pneumonic illness caused by bacterium *Legionella pneumophila*. *Legionella pneumophila* can be transmitted to humans via inhalation of contaminated aerosols generated by discharging showerheads.[1,2] Investigations showed that potable water was one of the most common exposure sources (16%) of a LD outbreak and accounted for 58-67% of outbreaks in buildings.[3] In Hong Kong, Legionellosis has been a reportable disease since 1994.[4] Among the recently reported LD cases, 4 (3–17.2 CFU ml^{-1}) out of 10 (3–72.4 CFU ml^{-1}) legionella-positive water samples were from bathroom showers.[5]

Like any other airborne disease, the infection of LD is affected by several factors, such as contaminated aerosol concentration, aerosol size distributions, breathing rate, exposure time and immunity,[6,7] in which for definite ventilation condition, the aerosol concentration in the space (e.g. bathroom) is related to aerosol generation rate of showerheads. Among these factors, size distribution of aerosols generated by discharging showerheads has been investigated in several studies.[1,8,9] Bollin et al. reported that approximately 90% (7 of 8 CFU) of the recovered aerosolized droplets containing *Legionella pneumophila* during showering were between 1 and 5 μm in diameter.[1] As Legionella is small enough to be enclosed inside the aerosolized droplets and the influence of Legionella on the droplet size is usually neglected. Xu and Weisel's study showed that 99.4% (by particle mass) shower-generated aerosols were larger than 0.2 μm.[8] Zhou et al.'s experimental study showed that the mass median diameter (MMD) of aerosols generated from showerheads running with hot water (43-44 ^{o}C) was 5.2-7.5 μm, while the aerosol size was 2.5-3.1 μm when running with cold water (24-25 ^{o}C).[9] It was found that aerosol size distribution varys with showerhead type, shower water temperature, flow rate, density (salt solution or not) and relative humidity of surrounding air.[1,8,9] Nevertheless, aerosols generated by showerheads raise concerns as they are small enough to penetrate deep into the lungs. As washroom is usually small, it can be assumed that the space is well-mixed/filled up entirely with aerosols. Therefore, aerosol concentration in bathroom is more important when considering the LD transmission, in which the aerosol concentration in bathroom is related to aerosol generation rate of showerheads. Among the several factors that influence the LD infection, this study focuses on the aerosol generation rate of showerheads only.

Installation of water efficient appliances is one demand-side water management policy that favored by water provides/water utilities managers.[10,11] In Hong Kong, in order to promote and help consumers choose low flow showerheads, a voluntary Water Efficiency Labelling Scheme (WELS) on showerheads for bathing has been proposed and implemented since

2009.[12] As low flow showerheads usually break up water into a fine mist which can be inhaled easily,[13] they enhance the transmission of LD. Hence, the installation of low flow showerheads brings new concerns related to aerosol generation rate by showerheads.

This study investigates experimentally the aerosol generation rates of four sample showerheads in a mechanically ventilated test chamber, assisted by computational fluid dynamics (CFD) simulations. The aerosol mass and particle generation rates are determined. Correlations between aerosol mass generation rate and showerhead attributes are analyzed, with expressions of aerosol generation rate by water supply pressure, spray jet momentum and nozzle area are proposed.

Literature review

Experiments of showerheads/taps discharging inside a chamber or bathroom/shower stall are widely used to investigate the aerosol generation.[6,9,14,15] Along with the experiments, aerosol mass or number balance equations in the test chamber or bathroom/shower stall were usually defined, in order to calculate the aerosol generation rate.[6,9,14] For the equation proposed by Carson, the aerosol loss caused by ventilation was included in the aerosol balance equation, while the aerosol deposition on chamber walls was not included, which caused the calculated aerosol generation rate less than the actual value.[6] For the mass balance equation in Cowen and Ollison's study, the term of first-order rate of decay was defined, but no specification about the cause of the decay.[14] In Zhou et al.'s work,[9] specific description of the first-order rate of decay was given; the aerosol loss was caused by the ventilation and the aerosol deposition on shower walls, floor and mannequin body, in which the aerosol deposition rate on shower walls was calculated based on mathematical expression given by Crump and Seinfeld.[16] However, in the result, only the total decay rate of aerosols was given, not specifying the value of the aerosol deposition rate. It can be seen that determining the aerosol deposition rate is necessary for the accurate estimation of aerosol generation rate. Except experimental methods, computational fluid dynamics (CFD) simulation is an alternative method for the study of aerosol deposition in the future, which has been used in many previous studies about indoor particulate contaminants.[17,18,19] Previous computational results revealed that indoor particulate concentration, distribution and deposition were related to the specific particulate properties, ventilation conditions and room dimensions. It is the same situation for aerosols in test chambers or shower stalls.

Considering the safety, salt was usually used to replace Legionella bacteria for experimental studies of aerosolized Legionella bacteria from water consuming appliances. Carson demonstrated that the use of salt to simulate the particulate Legionella may have effect on aerosol generation, but the effect was not significant.[6] Cowen and Ollison's study showed that introduction of salt solutions into the source water increased particle formation rates for size fractions < 10 µm, however, little apparent change in particle concentration for particles above 10 µm in size.[14] It was also pointed out that although salt content in water did has an influence on fine particle formation, the relationship was not linear over the tested total dissolved solids levels.[14]

For the correlations between aerosol generation rate and shower spray attributes, Carson reported that aerosol generation rate was linked to the smoothness of the flow stream.[6] Zhou et al. revealed that aerosol generation rate increased with showerhead water flow rate.[9] The impact of water temperature, flow rate and spray setting on aerosol formation was investigated by Cowen and Ollison, and it was revealed that although these parameters did have an effect on aerosol generation when within a single shower sampling run, no consistent effects for overall showerheads were found.[14] Even though several impact factors of aerosol generation for showerheads have been identified and investigated by these previous studies,[6,9,14] yet conclusive correlations are to be confirmed. Besides, the identified impact factors are limited, and many potential impact factors such as showerhead type, water supply pressure, water velocity and spray spread angle have not been evaluated.

Methodology

The methodology is divided into three parts, namely the experimental study of aerosol generation in a chamber, CFD simulation of aerosol deposition on chamber walls, and development of aerosol balance equation in the chamber. The logic of these three part is as shown in Figure 1, and details are described below.

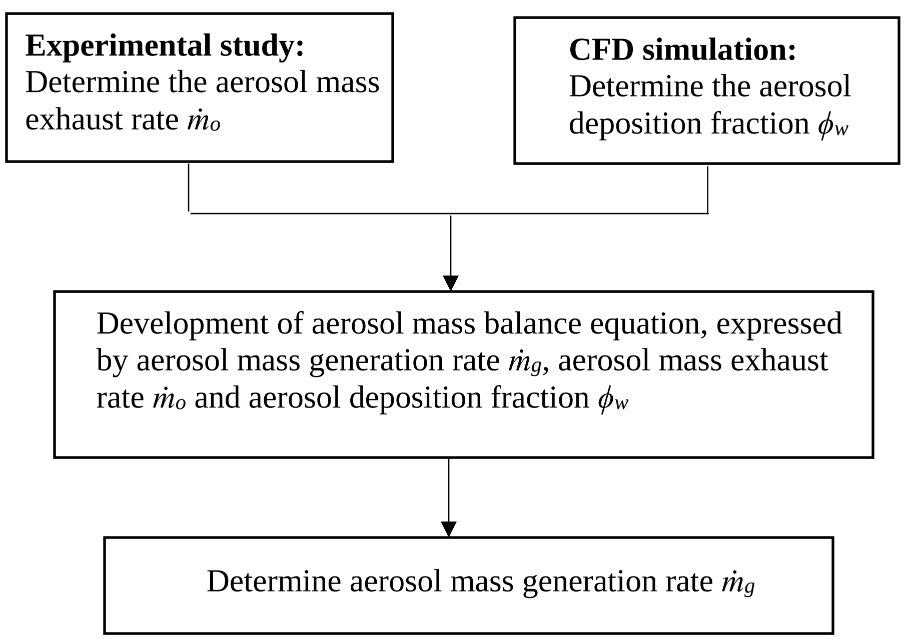

Figure 1. Logical diagram of the methodology.

Experimental study

Aerosol generation rates of sample showerheads were investigated experimentally in a glass chamber of size 0.914m×0.61m×0.508m, as shown in Figure 2. A small chamber was adopted so that more aerosols could be collected at the chamber outlet and hence to reduce the measurement time. The chamber was mechanically ventilated. An air filter was installed at the supply fan outlet, and the fan outlet was placed below the water level in the water tank. Air was filtered and moistened before supplying through the chamber inlet, which was 0.155 m in diameter, at a steady air velocity of 0.25 ms^{-1} (60 air changes per hour). The sample showerhead was fed from an enclosed tank filled with 2% saltwater solution (0.4 kg salt dissolved in 20 L distilled water) at pressure P_s (kPa), in which the pressure P_s is read from the pressure gauge installed in the water circulation system. The air fan, pressure gauge (range: 0 – 1400 kPa; accuracy: 20 kPa) and flow meter (accuracy: 0.1 L) installed in the experimental set-up are all common types.

In the experiment, a dry and clean filter paper with a pore size of 0.2 μm was placed at the chamber outlet to collect aerosolized saltwater for 3 hours (i.e. τ =10800 s). As one aim of this study is to quantify the aerosol mass generation rate and literature showed that shower-generated aerosols with size of less than 0.2 μm only contribute to approximately 0.6% of the total aerosol mass,[8] the filter paper with a pore size of 0.2 μm is thought enough for the aerosol collection in this study. The filter paper sample was then dried in an oven at 100ºC for 30 minutes (the baking time was determined according to no mass change of filter paper). As the total salt mass m_t (g) is the salt mass collected on the dried filter paper sample, the aerosol mass exhaust rate $\dot{m}_o$ can be determined by Equation (1), where ρ_d (=1000 kg m^{-3}) and ρ_t (=1020 kg m^{-3}) are the densities of water and saltwater respectively.

$$\dot{m}_o = ((\phi_t + 1)m_t)/\phi_t\tau \; ; \; \phi_t = (\rho_t - \rho_d)/\rho_d \tag{1}$$

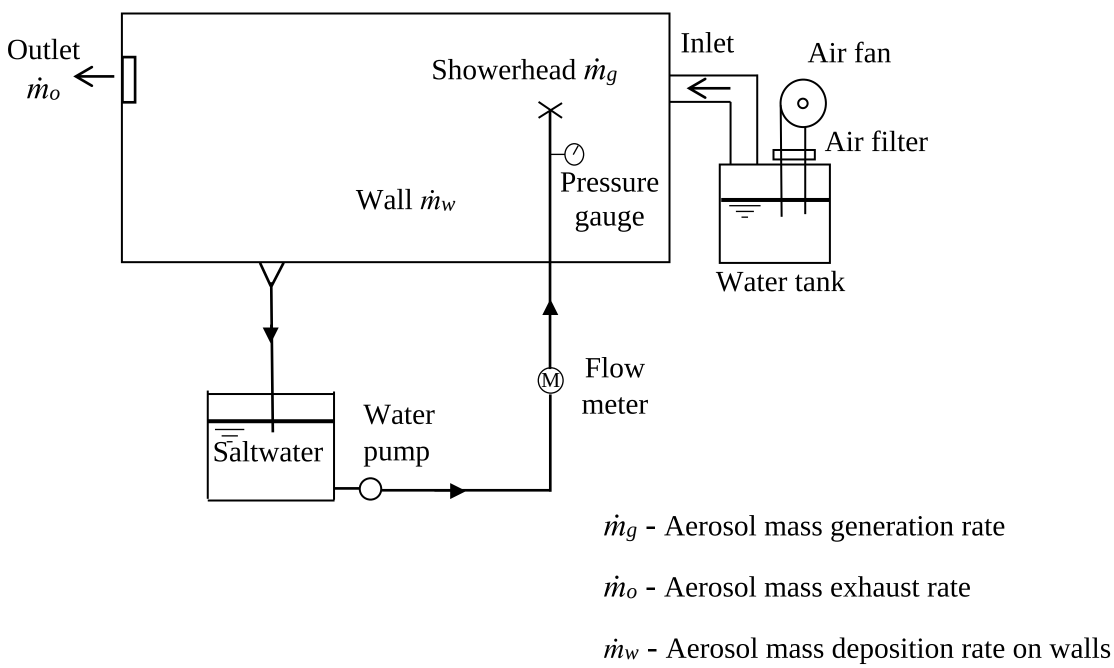

Figure 2. Experimental setup for showerhead aerosol generation study.

Computational fluid dynamics (CFD) simulation

The aerosol deposition fraction on chamber wall was acquired by CFD simulations.[20] Figure 3 shows a geometric model chamber that was built based on the experimental setup described above. As showerhead surface area is greatly less than the area of chamber walls, the aerosol deposition on showerhead surfaces is ignored in this study. Therefore, the showerhead can be represented by an aerosol generation source in the CFD simulation, and an absolute minimum size of the aerosol generation source is preferred in theory in order to avoid the deposition of aerosols on the surface of aerosol generation source. However, too much small size of aerosol generation source will cause the convergence difficulty for the CFD simulation. In this study, a cubic zone with size of 0.01m×0.01m×0.01m was used to represent the discharging showerhead in the chamber. The model chamber was automatically 'medium' meshed using the Relevance Center setting in ANSYS Fluent 13.0, and the suitability of the mesh size was verified by comparing simulated aerosol deposition fractions in different mesh sizes until there was no significant difference. Finally, 91007 calculation cells and 17449 nodes were set for the chamber.

Figure 3. Geometric model setup for CFD simulations.

The air phase motion was described by the Navier-Stokes equations, and a Lagrangian discrete phase model (DPM) was employed to separately track a number of stochastic aerosols from the source by solving the equations of aerosol motion. As the mass and momentum loadings of the aerosol phase were low in the chamber, uncoupled DPM was adopted, meaning that the aerosol motion was influenced by the air phase motion while the aerosol motion itself had no effect on the air phase motion. The number of stochastically tracked aerosols was verified by comparing with the ensemble average of the trajectories, namely simulated aerosol deposition fraction in this study. Finally, a statistical sample size of 12000 tracked aerosols was confirmed to represent the full range of aerosol behavior in this study.

For the simulation with Lagrangian DPM, the aerosol injection from the source was just at the beginning of the computation of the continuous phase (i.e. air phase). A velocity inlet boundary condition was chosen for inlet, and outflow boundary condition were set at the outlet. The chamber wall was the ‘stationary’ boundary condition. The discrete phase boundary condition type of both inlet and outlet was set as ‘escape’, and ‘trap’ discrete phase boundary condition was chosen for the chamber walls. Source was set as ‘reflect’ discrete phase boundary condition, and the refection coefficients in the normal and tangent directions were 1. Standard k-ε Model was adopted since it is proper for airflow simulation in the space and good agreement between simulation results and measured data has been achieved.[21] Besides, no aerosol aggregation and breakage were assumed.

At steady state, total tracked aerosols (i.e. 12000 tracers) is the sum of the aerosols deposited on chamber walls and exhausted from outlet. The number of aerosols that deposited on chamber walls n_w and exhausted from outlet n_o were acquired from the CFD simulation, and aerosol deposition fraction ϕ_w is determined by following expression,

$$\phi_w = \frac{n_w}{n_w + n_o} \tag{2}$$

For CFD model validation, another numerical simulation was performed with a chamber experimental setup by Carson, and the simulation results were compared with Carson's experimental results.[6] Figure 4 shows the geometric model setup used for the validation: test chamber size is 1.53×0.84×0.835m; sink size is 0.4×0.33×0.17 m (the sink is located at the bottom of the chamber); circular air inlet and outlet are both 0.15 m in diameter; a flat rectangular blade (0.1×0.02×0.005 m) represents a mixing fan; a cylindrical zone of 0.12 m in diameter and 0.025 m in height is set for fan rotation in the simulations; and a cubic zone (0.01m×0.01m×0.01m) represents the aerosol generation source (i.e. discharging tap/showerhead). Aerosol concentrations at the sampling point were determined from the simulation. It should be noted that the sampling point was the reference aerosol sampling location in the Carson's experiment.[6]

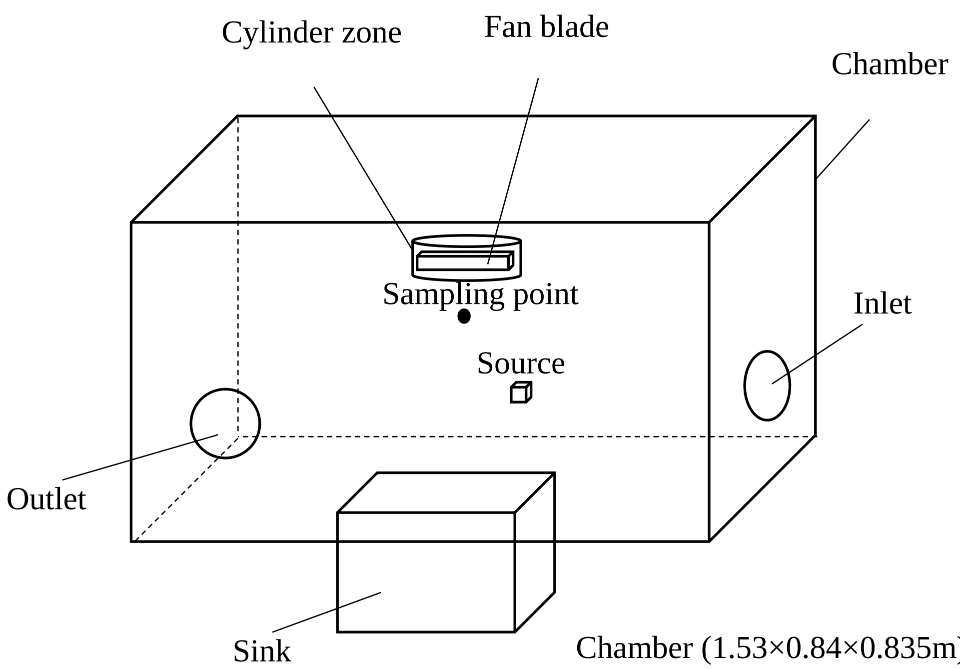

Chamber (1.53×0.84×0.835m)
Sink (0.4×0.33×0.17m)
Inlet (diameter D_i = 0.15m)
Outlet (diameter D_o=0.15m)
Fan blade (0.1×0.02×0.005m)
Cylinder zone (base diameter D = 0.12 m, height H = 0.025m)
Source (0.01×0.01×0.01m)

Figure 4. Geometric model setup for CFD simulations (for validation study).

In the validation study, an Euler-Euler multiphase model was adopted to determine the airflow field and aerosol concentration in the chamber. The renormalization group (RNG) k-ε model was selected to include the effect of swirl on turbulence, while standard wall functions were applied to the near-wall region. The air and aerosols were treated as interpenetrating continua and no slip velocity between air phase and fine aerosol particle phase was assumed. Partial equilibrium of pressure gradient and gravity was taken into account in the momentum equation for the air-aerosol mixture.

The aerosol was characterized as a salt water droplet with density of 1018 kg m^{-3} and diameter of 4.94μm in the mixture model. Aerosols were injected into the chamber from the generation source continuously. A velocity inlet boundary condition was set at the inlet with initial air and aerosol velocities of 0.67 m s^{-1} and 0 m s^{-1} respectively. As there were no aerosols flowing into the chamber from the inlet, the aerosol volume fraction at the inlet was set as zero. An effective outflow boundary condition was chosen for the outlet, and the aerosol generation source was set as the mass flow inlet boundary condition. The mass flow rates of air and aerosols at the aerosol generation source were 0 kg s^{-1} and 1.5×10^{8} kg s^{-1} respectively.

Four rotational speeds of the fan were set in the CFD simulations, i.e. 1000 revolutions per minute (rpm), 2000 rpm, 3000 rpm and 4000 rpm, and no heat transfer was considered in the numerical simulation. Table 1 outlines the parameters adopted in the simulations.

Table 1. Parameters involved in the CFD simulations.

Zone	Boundary condition	Parameter	Unit	Value	Remark
-	-	Ventilation rate Q_v	$m^3\,s^{-1}$	0.0119	Carson (1996)
-	-	Aerosol diameter d_{pr}	m	4.94×10^{-6}	Carson (1996)
-	-	Aerosol density ρ_{pr}	$kg\,m^{-3}$	1018	Carson (1996)
-	-	Aerosol generation rate $\dot{n}_{pr}$	Particles s^{-1}	2.34×10^5	Carson (1996)
-	-	Rotational velocity of moving reference frame ω_r	rpm	1000/2000/3000/4000	-
Inlet	velocity inlet	Air velocity $v_{i,a}$	$m\,s^{-1}$	0.67	$v_{i,q}=Q/(\pi \varnothing_i^2/4)$ Mixture model
		Aerosol velocity $v_{i,pr}$	$m\,s^{-1}$	0	Mixture model
		Aerosol volume fraction δ_{pr}	-	0	Mixture model
Outlet	outflow	-	-	-	Mixture model
Source	mass flow inlet	Air mass flow rate $Q_{m,a}$	$kg\,s^{-1}$	0	Mixture model
		Aerosol mass flow rate $Q_{m,pr}$	$kg\,s^{-1}$	1.5×10^{-8}	$Q_{m,pr}=(4/3)\pi(d_{pr}/2)^3\rho_{pr}n_{pr}$ Mixture model
Fan blade	moving wall	Relative rotational velocity ω_{relat}	rpm	0	Mixture model
Chamber, sink wall	stationary wall	-	-	-	Mixture model

Aerosol mass balance model in the chamber

Inside a well-mixed ventilated chamber, the aerosol concentration of a generation source is given by the aerosol mass balance as expressed in Equation (3), where $\dot{m}_c$ (gs^{-1}) is the aerosol mass change rate, $\dot{m}_g$ (gs^{-1}) is the aerosol mass generation rate, $\dot{m}_i$ (gs^{-1}) is the aerosol mass inflow rate, $\dot{m}_o$ (gs^{-1}) is the aerosol mass exhaust rate, and $\dot{m}_w$ (gs^{-1}) is the wall deposition rate of the aerosol mass.

$$\dot{m}_c = \dot{m}_g + \dot{m}_i - \dot{m}_o - \dot{m}_w \tag{3}$$

Let the aerosol deposition fraction on the chamber walls be $\phi_w = \dot{m}_w / \dot{m}_g$, the aerosol mass generation rate at steady state (i.e. $\dot{m}_c = 0$) and without any aerosols from inflow (i.e. $\dot{m}_i = 0$) is given by,

$$\dot{m}_g = \dot{m}_o + \dot{m}_w = \dot{m}_o / (1 - \phi_w) \tag{4}$$

The aerosol mass exhaust rate $\dot{m}_o$ in Equation (4) can be determined in the experimental study while the aerosol deposition fraction on the chamber walls ϕ_w can be acquired from the CFD simulations above.

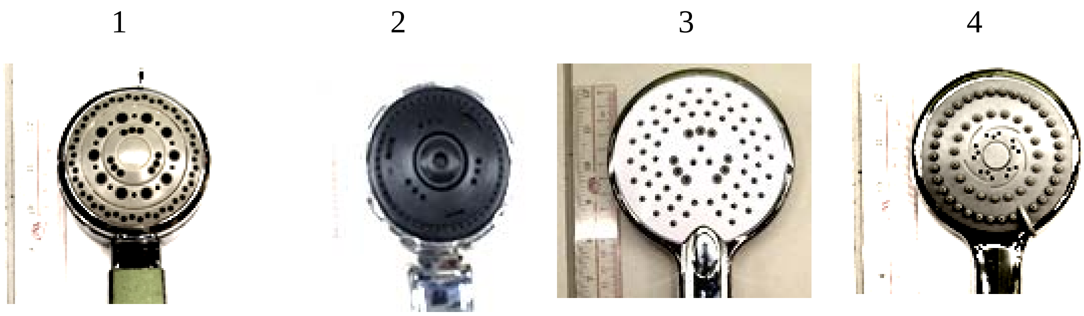

Figure 5. Sample showerheads.

Sample showerheads

Figure 5 shows the four sample showerheads adopted in this study. Samples 3 and 4 were WELS labelled Grade 1 showerheads with reduced nominal flow rates.[12] The physical properties of all sample showerheads are summarized in Table 2. The selected four sample showerheads cover a wide range of primarily operating characteristics, e.g. pressure, resistance factor K_s and flow rate. It should be noted that Grade 1 showerheads still get a wide range of products. The experiment here is intent to cover a wider range of conditions, therefore the choice of the sample showerheads is as this. The nozzle area ratio ϕ_A is expressed by the total nozzle area A_s (m^2) on the showerhead faceplate divided by the faceplate area A_f (m^2),

$$\phi_A = \frac{A_s}{A_f} \tag{5}$$

Shower spray attributes were measured by a laboratory-made water circulation system, as shown in Figure 6. A pressure gauge and a water meter were installed in the system, which are all common types. An annular gauge was placed 0.4m below the showerhead to measure the water distribution patterns within the spray cross-section. As shown in Figure 7, the annular gauge had four concentric circular arrays of graduated cylinders. A high speed camera (model: FPS1000; takes from 840 to over 10000 frames per second) was placed aside for taking photos of showerhead discharging.

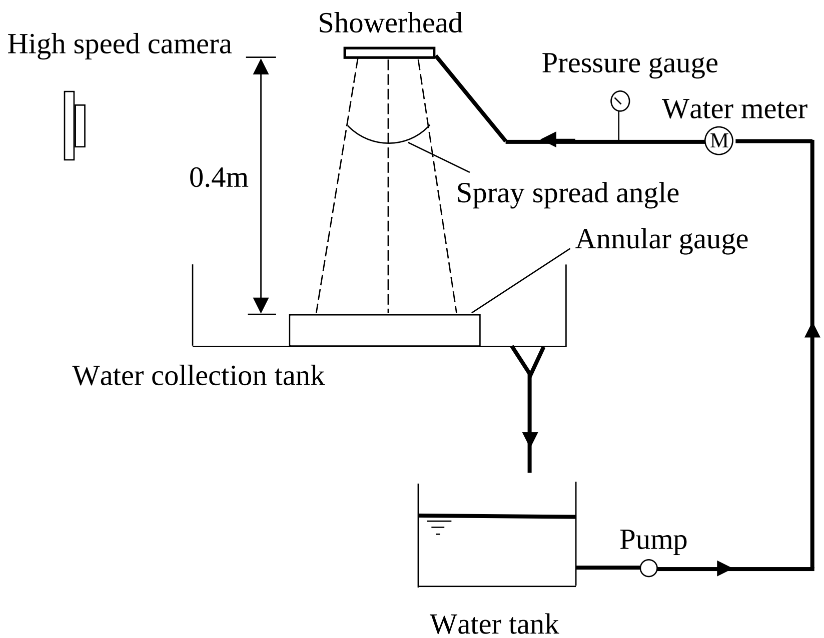

Figure 6. Experimental set-up for measurement of shower spray attributes.

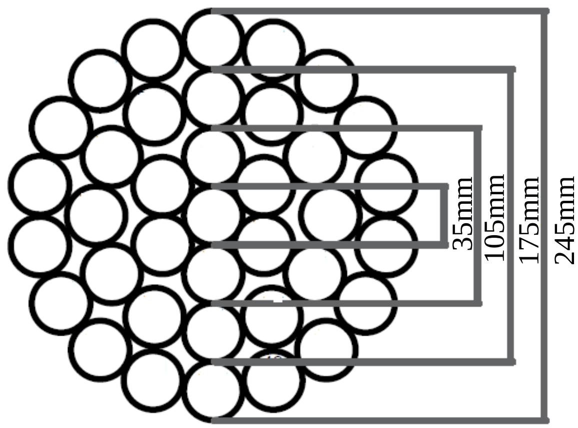

Figure 7. Annular gauge.

The discharged water volume of a sample operation of about 20s was read from the water meter and the average water flow rate of a showerhead Q_s was determined from the water volume divided by the operation time. Water flow rates under pressure range of 50-250 kPa were measured.

Local loss at showerhead is usually calculated by Equation (6), where P_s (kPa) is the water supply pressure, ζ is the loss coefficient, Q_s (L s^{-1}) is the water supply flow rate, and g (ms^{-2}) is the gravitational force.[15]

$$P_s = \zeta \frac{Q_s^{\ 2}}{2g} \tag{6}$$

Defining showerhead resistance factor $K_s = \zeta/2g$, Equation (6) is rewritten as,

$$P_s = K_s Q_s^{\ 2} \tag{7}$$

Therefore, the sample showerhead resistance factor K_s (kPa min^2 L^{-2}) can be calculated using the water supply pressure P_s (kPa), which is in a pressure range between 50 kPa and 250 kPa, and the water supply flow rate Q_s (L s^{-1}),

$$K_s = \frac{P_s}{\left(Q_s/60\right)^2} \tag{8}$$

While the spray spread angle θ_s (°) and spray jet velocity v_s (ms^{-1}) can be determined from the captured images of a high-speed camera, the spray jet momentum M_s (m^4 s^{-2}) is expressed by,[22]

$$M_s = Q_s v_s \tag{9}$$

Moreover, the water spray uniformity ϕ_u is expressed by Equation (10), where $u_{s,d}$ (L s^{-1} m^{-2}) is the mass flux density at a distance from the centerline of the showerhead d_s (m), as shown in Figure 8, $A_{s,d}$ (m^2) is the water collection area of an annular gauge, and $Q_{s,d}$ (L s^{-1}) is the water spray flow rate determined from the water collected over a period of 20 s.

$$\phi_u = \frac{\bar{u}}{u_{\max}}\,;\; \bar{u} = \frac{\sum Q_{s,d}}{\sum A_{s,d}}\,;\; u_{s,d} = \frac{Q_{s,d}}{A_{s,d}} \tag{10}$$

The annular gauges shown in Figure 6 can be replaced by an electronic scale to measure the spray jet force. The spray jet force F_s (N) is calculated by Equation (11), where m_r (kg) is the mass reading from the electronic scale when the showerhead is operating, m_0 (kg) is the mass of the water left on the electronic scale after showering and g (m s^{-2}) is the gravitational force.

$$F_s = (m_r - m_0)g \tag{11}$$

The spray jet force can also be expressed by spray attributes as given by Equation (12), where m_s is the water spray mass flow rate, a_s is the spray jet acceleration, ρ_t is the spray water density, $v_{s,h}$ is the spray jet velocity at a vertical distance of h below the showerhead, and τ is the time taken for the jet spray from the showerhead faceplate to reach h.

$$F_s = m_s a_s\,;\; m_s = Q_s \rho_t\,;\; a_s = \frac{v_{s,h} - v_s}{\tau} \tag{12}$$

Table 2. Showerhead physical properties, spray attributes and aerosol generation rates.

Parameter	Sample showerheads			
	1	**2**	**3[a]**	**4[a]**
Showerhead				
Diameter, D_s (m)	0.080	0.045	0.115	0.085
Number of 1/2/3 mm nozzles, $n_1/n_2/n_3$	48/19/10	48/9/0	59/9/0	53/15/0
Nozzle area ratio, ϕ_A	0.0334	0.0415	0.0072	0.0156
Resistance factor, K_s (kPa min^2 L^{-2})	1.82	1.90	16.50	3.36
Shower water spray measured at P_s=100 kPa (at 150 kPa)				
Flow rate, Q_s (L s^{-1})	0.13 (0.16)	0.12 (0.14)	0.04 (0.05)	0.10 (0.12)
Spray spread angle, θ_s (º)	11 (11)	2 (2)	11 (11)	9 (9)
Spray jet velocity, v_s (m s^{-1})	0.77 (0.95)	1.82 (2.12)	0.56 (0.70)	1.13 (1.35)
Momentum, M_s (×10^{-4} m^4 s^{-2})	1.01 (1.52)	2.18 (2.97)	0.24 (0.36)	1.13 (1.62)
Uniformity, ϕ_u	0.21 (0.62)	5.95 (0.58)	0.68 (0.52)	0.33 (0.51)
Spray jet force, F_s (N)	0.75 (1.06)	1.05 (1.32)	0.34 (0.44)	0.62 (0.98)
Aerosol mass generation rate, $\dot{m}_g$ (×10^{-5} gs^{-1})	2.85 (3.92)	3.03 (5.52)	1.42 (3.03)	2.14 (3.38)

[a]WELS labelled Grade 1 showerhead.

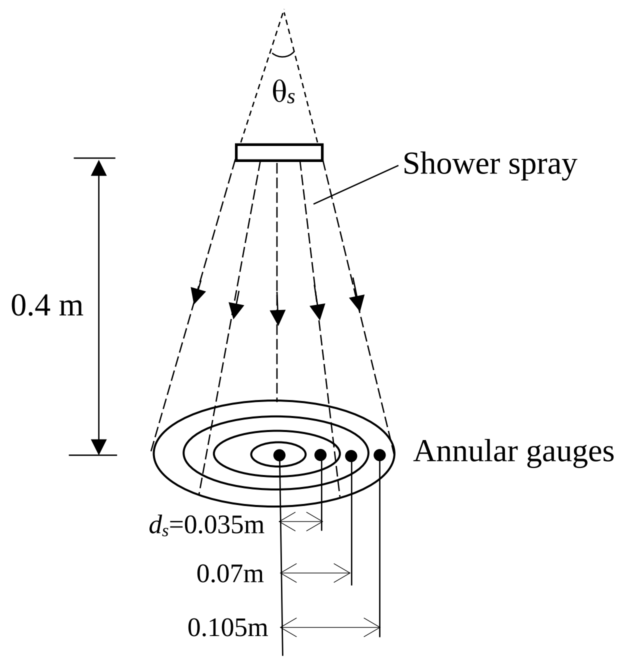

Figure 8. Spray spread angle and water distribution patterns.

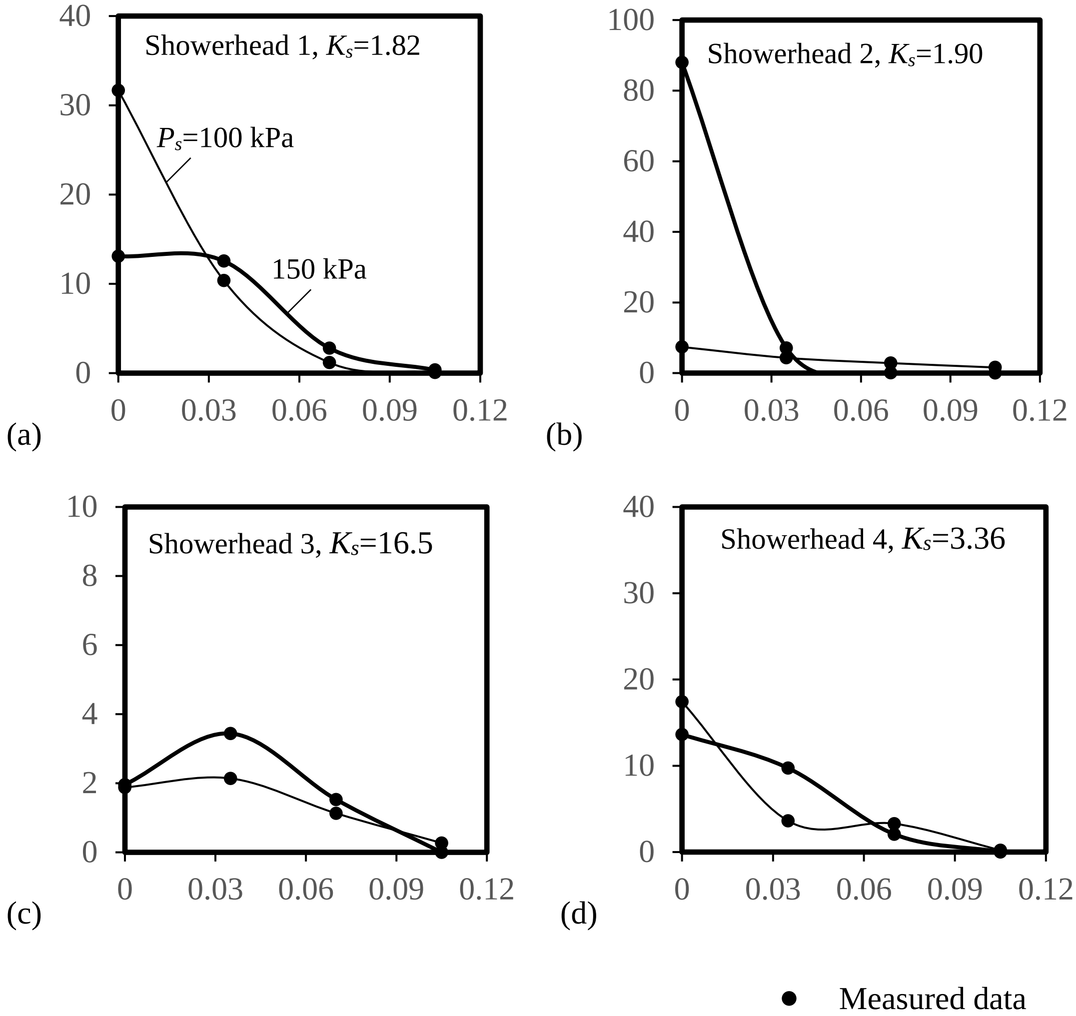

x-axis: Distance from showerhead d_s (m); y-axis: Mass flux density $u_{s,d}$ (L s^{-1} m^{-2})

Figure 9. Measured mass flux densities for 4 sample showerheads.

Results and discussions

Figure 9 shows the mass flux density ($u_{s,d}$) measurement results for the four sample showerheads. Although Showerheads 1 and 2 had similar resistance factors (i.e. 1.82 and 1.90 kPa min^2 L^{-2}), they had very different water discharge patterns. For a water supply pressure varied from 100 kPa to 150 kPa, Showerhead 1 gave a concentrated mass flux in the near axial distance at a lower pressure and a more evenly distributed mass flux over the spray coverage at a higher pressure while Showerhead 2 gave opposite results. Using the absolute gradient $\phi_u' = \left|\frac{d\phi_u}{dP_s}\right|$ to indicate the pressure sensitivity of the water distribution patterns, the distribution patterns of the WELS labelled Showerheads 3 and 4 (ϕ_u'=0.003 and 0.004 respectively) were found to be less sensitive to water supply pressure as compared with Showerheads 1 and 2 (ϕ_u'= 0.008 and 0.11 respectively). In general, Showerheads 3 and 4 gave more even discharge patterns over the spray coverage and their uniformities were less sensitive to the water supply pressure.

For the CFD model validation, the simulated value of aerosol concentration with a fan speed of 2000rpm at the sampling point was 1.89×10^7 particles m^{-3}, and that was very close to the value found in Carson's experiment (1.97×10^7 particles m^{-3}).[6] Based on the setting in the CFD models that the aerosol motion had no effect on the air phase motion and there was no slip velocity between air phase and aerosol particle phase, it can be seen that the aerosol tracks were totally dependent on the air motion paths. The CFD models that govern the air-aerosol flow in chambers were validated. This also implies that, together with the aerosol tracking model (i.e. Lagrangian discrete phase model (DPM) in this study), the CFD models that govern the air-aerosol flow in chambers can be used directly for the aerosol tracking (deposition) study.

Among the total number of tracked aerosols (i.e. n_w+n_o=12000), n_w=8933 aerosols were trapped on the chamber walls, corresponding to an aerosol deposition fraction on the chamber walls ϕ_w=0.74. Double tracked aerosol number (i.e. n_w+n_o=24000) was tried, and same aerosol deposition fraction on the chamber walls was found (i.e. ϕ_w=0.74). This implies that: (1) the 12000 tracers can represent the full aerosol behavior range in this study; and (2) aerosol deposition fraction on the chamber walls is independent of aerosol generation rate. The aerosol deposition is related to the specific aerosol properties, ventilation conditions and chamber dimensions. Aerosol deposition fraction ϕ_w=0.74 is for the case in this study.

Table 2 shows that aerosol mass generation rate increased with water supply pressure at showerhead. The ratios of aerosol mass generation rate to water supply pressure for the four sample showerheads were plotted in Figure 10, in which a reference line indicates perfectly linear increase of aerosol generation rate with water supply pressure at showerhead. By defining acceptable error range, linear increase of aerosol generation rate with water supply pressure at showerhead can be concluded from Figure 10.

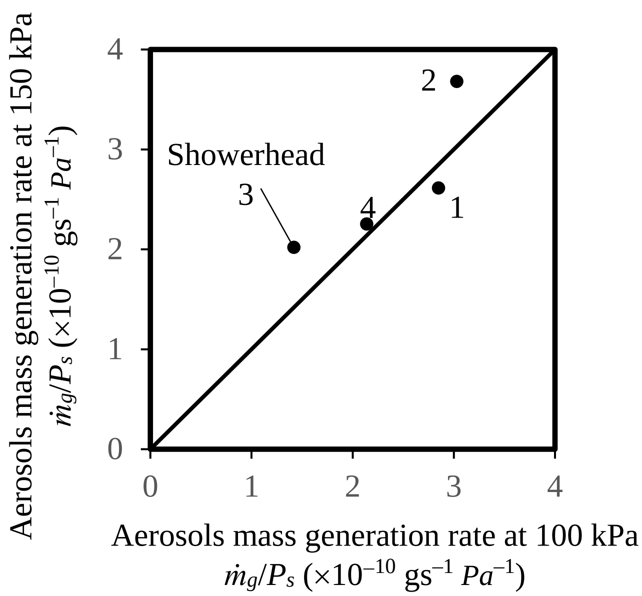

Figure 10. Ratio of aerosol mass generation rate to water supply pressure at showerhead

Figures 11(a) to 11(g) illustrate the ratio of aerosol mass generation rate to water supply pressure $\dot{m}_g/P_s$ ($\times 10^{-10}$ gs^{-1} Pa^{-1}) against the nozzle area ratio ϕ_A, showerhead resistance factor K_s (kPa min^2 L^{-2}), water supply flow rate Q_s (L s^{-1}), spray jet velocity v_s (m s^{-1}), spray jet momentum M_s (m^4 s^{-2}), uniformity ϕ_u and spray jet force F_s (N) respectively. All parameters except uniformity show a significant correlation with the aerosol mass generation rate ($p \leq 0.05$, t-test). As shown in Figures 11(a) to 11(e) and Figure 11(g), the aerosol mass generation rate decreases with the showerhead resistance factor but increases with the water supply pressure, nozzle area ratio, flow rate, spray jet velocity, momentum and force. While water supply pressure, nozzle area ratio, flow rate, spray jet velocity and momentum are all related to the showerhead itself, spray jet force is exerted by the spray-surface interaction. The spray jet force is an indicator of the splashing effect caused by water spray jet impaction on a surface; a greater force produces a greater splashing effect and thus more aerosols.

The relationship between aerosol mass generation rate and showerhead attributes can be expressed by,

$$\dot{m}_g/P_s \sim (\phi_A, K_s, Q_s, v_s, M_s, F_s);\ M_s \sim (Q_s, v_s);\ K_s \sim (P_s, Q_s);\ F_s \sim (Q_s, v_s) \qquad (13)$$

It can be rewritten as,

$$\dot{m}_g/P_s \sim (\phi_A, M_s) \qquad (14)$$

Equations for the trend lines in Figure 11(a) and Figure 11(e) were given as following,

$$\dot{m}_g/P_s = 1\times10^{-4}\phi_A^{0.36};\ \dot{m}_g/P_s = 0.004M_s^{0.3} \qquad (15)$$

As Equation (15) shows that $\dot{m}_g/P_s \sim \phi_A{}^{0.36}$ and $\dot{m}_g/P_s \sim M_s{}^{0.3}$, the aerosol mass generation rate $\dot{m}_g/P_s$ against $M_s{}^{0.3}\phi_A{}^{0.36}$ was plotted in Figure 12 for analysis. Figure 12 gives the expression of aerosol mass generation rates $\dot{m}_g$ (gs^{-1}) by water supply pressure, spray jet momentum and nozzle area ratio, with p=0.001 (t-test).

$$\dot{m}_g = 0.00022 P_s M_s{}^{0.16} \phi_A{}^{0.19} \tag{16}$$

As the results are from the test range, which delinked from the graded showerheads. Therefore, Equation (16) can be the referenced guidance for future showerhead design to limit the aerosol generation rate.

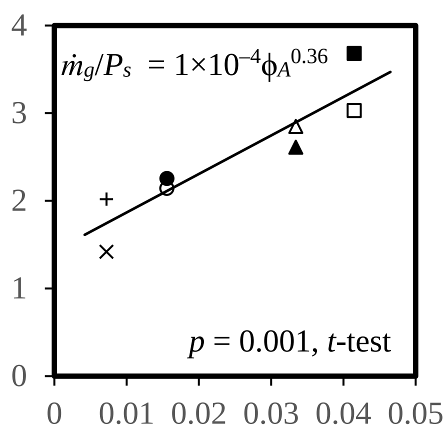

(a) Nozzle area ratio ϕ_A

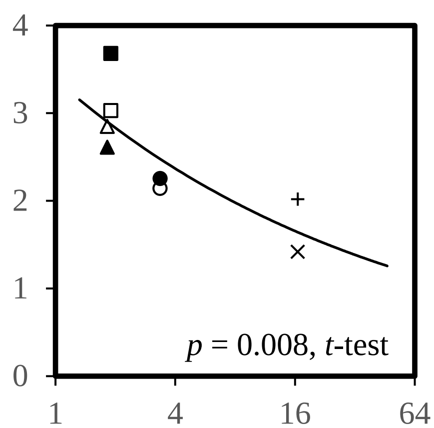

(b) Resistance factor K_s (kPa min^2 L^{-2})

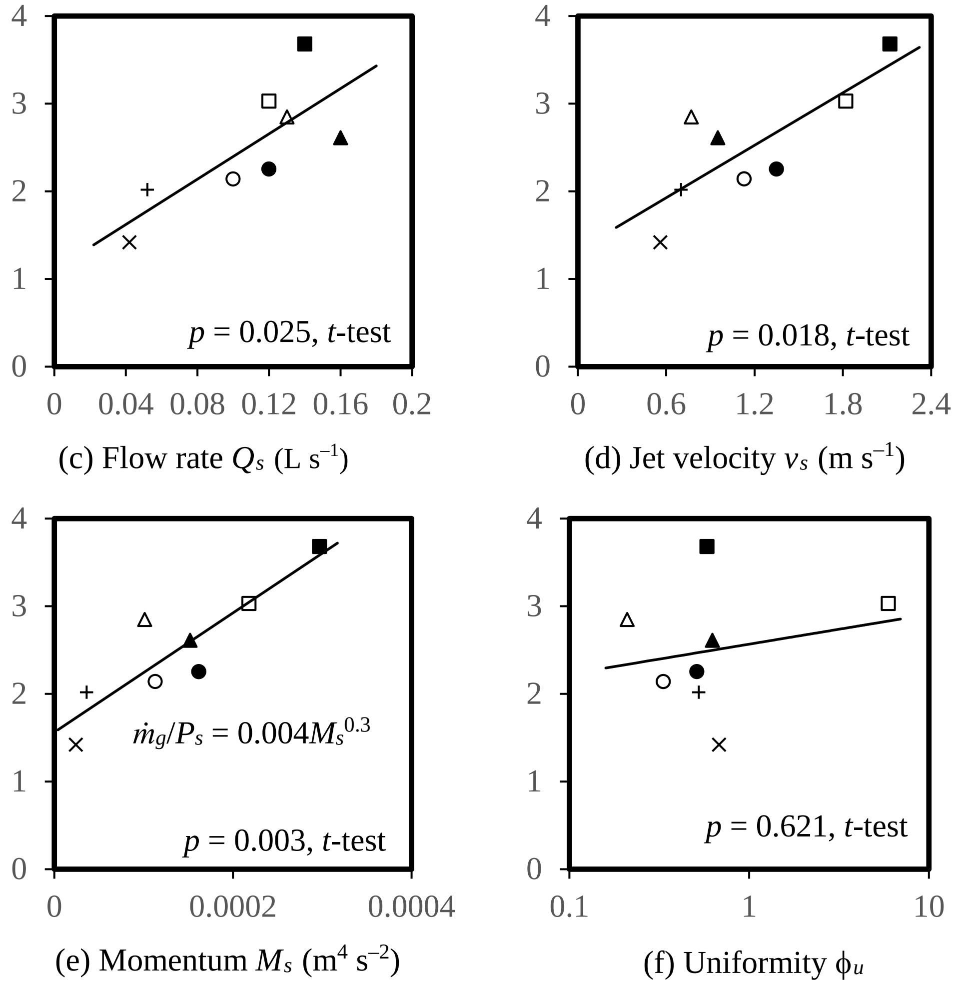

p = 0.025, t-test
(c) Flow rate Q_s (L s^{-1})
p = 0.018, t-test
(d) Jet velocity v_s (m s^{-1})
$\dot{m}_g/P_s = 0.004M_s^{0.3}$
p = 0.003, t-test
(e) Momentum M_s (m^4 s^{-2})
p = 0.621, t-test
(f) Uniformity ϕ_u

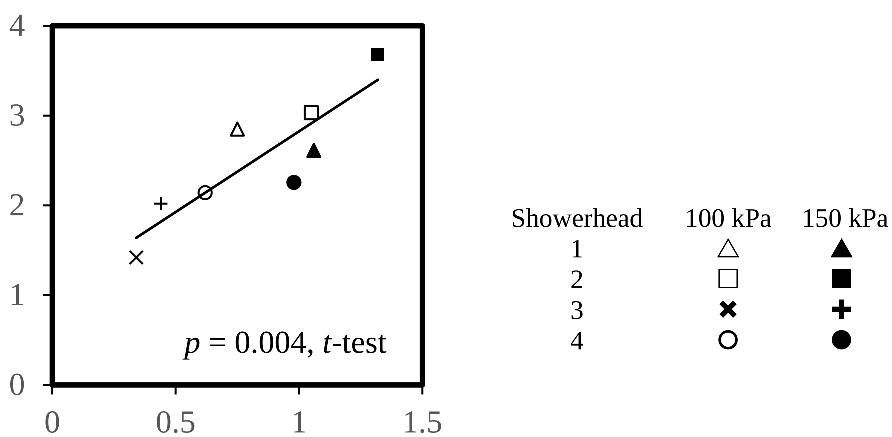

(g) Spray force F_s (N)

y-axis: Aerosol mass generation rate $\dot{m}_g/P_s$ ($\times 10^{-10}$ gs^{-1} Pa^{-1})

Figure 11. Correlations for aerosol mass generation rate.

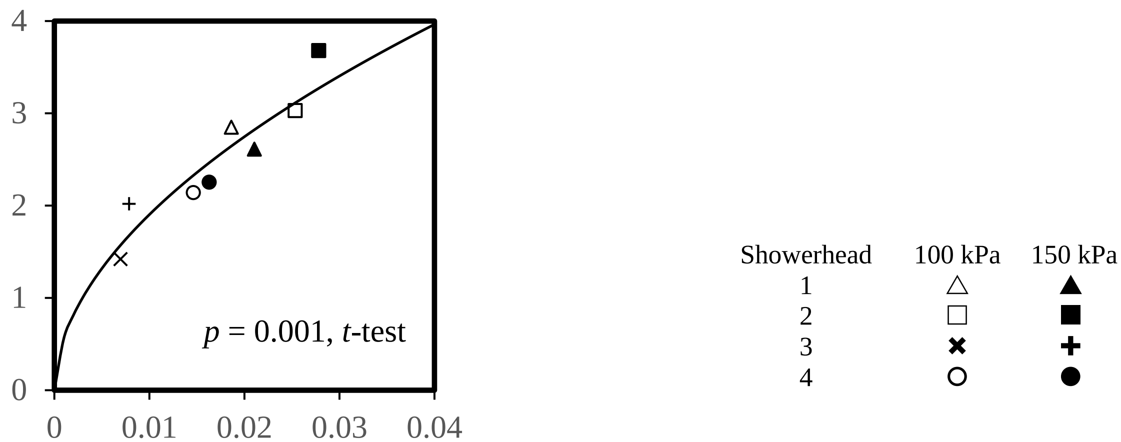

x-axis: $M_s^{0.3}\phi_A^{0.36}$; y-axis: Aerosol mass generation rate $\dot{m}_g/P_s$ ($\times 10^{-10}$ gs^{-1} Pa^{-1})

Figure 12. Aerosol mass generation rate as a function of $M_s^{0.3}\phi_A^{0.36}$.

Average diameter (=4.25 μm) of aerosols generated from showerheads was determined according to the studies by Bollin et al.[1] and Zhou et al.[9], then corresponding volume of an aerosol V_s (=40.17 μm^3) was calculated. The aerosol particle generation rates $\dot{n}_g$ (particles s^{-1}) of the sample showerheads can be given by Equation (17). Results show that aerosol particle generation rate for the four sample showerheads ranged from 0.35×10^6 particles s^{-1} to 1.35×10^6 particles s^{-1}. Compared with the previous experimental results for taps (=0.234×10^6 particles s^{-1}) reported by Carson,[6] the results validate the assumption that showerheads generate more aerosols than water taps as showerheads have more holes on faceplate.

$$\dot{n}_g = 10^{15}\dot{m}_g/\rho_t V_s \tag{17}$$

Table 2 shows that when all sample showerheads were operating at the same pressure, the aerosol generation rates of the WELS labelled Showerheads 3 and 4 were less than those of Showerheads 1 and 2. Our previous study[23] revealed that the optimum pressure of WELS labelled showerheads was larger than that of conventional showerheads; however, the aerosol generation rate of a WELS labelled showerhead can still be controlled by the adjustment of momentum M_s and nozzle area ratio ϕ_A as demonstrated by Equation (16).

As shown in Table 2, low flow Showerheads 3 and 4 have less large holes on the showerhead faceplate compared with Showerhead 1 and 2. It can be seen that the two sample low flow showerheads in this study were achieved by reducing average hole size. There is also another type of low flow showerhead which induces air into showerhead,[24] that is not included in this study. This type of low flow showerhead mixes air with water to enlarge water droplet, corresponding a fine mist may be caused, and further aerosol generation rate may be increased. Besides the parameters shown in Equation (16) (i.e. water supply pressure at showerhead P, spray jet momentum M_s and nozzle area ratio ϕ_A), for future studies, parameters of induced air flow rate, air volume, and air pressure should be considered when investigating the aerosol generation rate of low flow showerheads of air-water mixing type. Moreover, the influence of water hardness and scale formation on aerosol generation of showerheads is not considered in this study, which may need further investigation in future research.

Conclusion

Aerosolization of water from discharging water appliances provides a transmission medium for Legionnaires' disease. In this study, the aerosol generation rates of four sample showerheads in a mechanically ventilated test chamber were investigated experimentally, assisted by CFD simulations. The aerosol mass generation rates and aerosol particle generation rates determined for the sample showerheads were in the ranges of 1.42×10^{-5} to 5.52×10^{-5} gs^{-1} and 0.35×10^{6} to 1.35×10^{6} particles s^{-1} respectively. The results showed that aerosol mass generation rate decreased with the showerhead resistance factor but increased with the water supply pressure, nozzle area ratio, flow rate, spray jet velocity, momentum and force. No significant correlation was found between aerosol mass generation rate and water spray uniformity ($p>0.05$, *t*-test). Furthermore, an expression of aerosol mass generation rate by water supply pressure at showerhead, spray jet momentum and nozzle area ratio was proposed, which can be used as a referenced guidance for the showerhead design to limit the aerosol generation rate. It was also reported that the low flow showerheads generated fewer aerosols while operating at the same pressure as conventional showerheads.

Acknowledgments

The work described in this paper was partially supported by a grant from the Hong Kong Research Grants Council (PolyU 5272/13E) and by three grants from The Hong Kong Polytechnic University (GYBA6, GYM64, GYBFN).

Author Contributions

Ling-tim Wong and Kwok-wai Mui were the study coordinators and involved in the data analysis and result reporting. Pak-hei Tsui, Wing-ki Chan and Yang Zhou conducted the experiment. Yang Zhou also performed the simulations.

References

1. Bollin GE, Plouffe JF, Para MF and Hackman B. Aerosols containing Legionella Pneumophila generated by shower heads and hot-water faucets. *Applied and Environmental Microbiology* 1985; 1128-1131.
2. Fields BS, Benson RF and Besser RE. Legionella and Legionnaires' disease: 25 years of investigation. *Clinical Microbiology Reviews* 2002; 15:506-26.
3. Garrison LE, Kunz JM, Cooley LA, et al. Vital signs: Deficiencies in environmental control identified in outbreaks of Legionnaires' disease – North America, 2000-2014, https://www.cdc.gov/mmwr/volumes/65/wr/mm6522e1.htm (accessed 7 July 2016).
4. Berger S. *Legionellosis: global status*. Los Angeles: Gideon, 2017.
5. Hong Kong Government. Press Releases: Update on cases of legionnaires' disease, http://www.info.gov.hk/gia/general/201612/28/P2016122800608.htm (2016, accessed 5 April 2017).
6. Carson W. Aerosol generation by taps and the resultant exposure of humans to Legionella bacteria. *Proceedings of CIB commission W062*, 1996.
7. Kowalski W. *Aerobiological Engineering Handbook: A guide to airborne disease control technologies*. The McGraw-Hill Companies, Inc. USA., 2006, pp. 42-43.
8. Xu X, Weisel CP. Inhalation exposure to haloacetic acids and haloketones during showering. *Environmental Science & Technology* 2003; 37(3):569-576.

9. Zhou Y, Benson JM, Irvin C, et al. Particle size distribution and inhalation dose of shower water under selected operating conditions. *Inhalation Toxicology* 2007; 19:333-342.

10. Millock K, Nauges C. Household adoption of water-efficient equipment: The role of soci-economic factors, environmental attitudes and policy. *Environmental and Resource Economics* 2010; 46:539-565.

11. Price JI, Chermak JM, Felardo J. Low-flow appliances and household water demand: An evaluation of demand-side management policy in Albuquerque, New Mexico. *Journal of Environmental Management* 2014; 133:37-44.

12. Wong LT, Mui KW, Zhou Y. Impact evaluation of low flow showerheads for Hong Kong residents. *Water* 2016; 8(7):305-316.

13. U.S. Department of Energy. Energy Saver, http://energy.gov/energysaver/reduce-hot-water-use-energy-savings (accessed 12 July 2016).

14. Cowen KA, Ollison WM. Continuous monitoring of particle emissions during showering. *Journal of the Air & Waste Management Association* 2006; 56(12):1662-1668.

15. O'Toole J, Keywood M, Sinclair M, et al. Risk in the mist? Deriving data to quantify microbial health risks associated with aerosol generation by water-efficient devices during typical domestic water-using activities. *Water Science and Technology* 2009; 60(11):2913-2920.

16. Crump JG, Seinfeld JH. Turbulent Deposition and Gravitational Sedimentation of an Aerosol in a Vessel of Arbitrary Shape. *Journal of Aerosol Science* 1981; 12(5):405-415.

17. Lu WZ, Howarth AT. Numerical analysis of indoor aerosols particle deposition and distribution in tow-zone ventilation system. *Building and Environment* 1996; 31(1):41-50.

18. Zhao B, Zhang Y, Li XT, et al. Comparison of indoor aerosol particle concentration and deposition in different ventilated rooms by numerical method. *Building and Environment* 2004; 39:1-8.

19. Chang TJ, Hsieh YF, Kao HM. Numerical investigation of airflow pattern and particulate matter transport in naturally ventilated multi-room buildings. *Indoor Air* 2006; 16:136-152.

20. ANSYS Fluent Theory Guide. Release 15.0, November 2013.

21. Stamou A, Katsiris I. Verification of a CFD model for indoor airflow and heat transfer. *Building and Environment* 2006; 41:1171-1181.

22. Thomas JD, Liu CM, Flachskampf FA, et al. Quantification of jet flow by momentum analysis. *Circulation* 1990; 81(1).

23. Chan WK, Wong LT, Zhou Y, Mui KW. An experimental study of shower spray properties and shower comfort. *The International Conference on Energy Engineering and Environmental Protection*, Xiamen, China, 16-18 December 2016.

24. Toyosada K, Otani T, Shimizu Y, et al. Research on the effect of showerhead characteristics on usage time and hot water volume. *The 39th International Symposium of CIB W062 Water Supply and Drainage for Buildings*, Nagano, Japan, 17-20 September 2013.

Table/ Figure legends

Figure 1. Logical diagram of the methodology.

Figure 2. Experimental setup for showerhead aerosol generation study.

Figure 3. Geometric model setup for CFD simulations.

Figure 4. Geometric model setup for CFD simulations (for validation study).

Figure 5. Sample showerheads.

Figure 6. Experimental set-up for measurement of shower spray attributes.

Figure 7. Annular gauge.

Figure 8. Spray spread angle and water distribution patterns.

Figure 9. Measured mass flux densities for 4 sample showerheads.

Figure 10. Ratio of aerosol mass generation rate to water supply pressure at showerhead

Figure 11. Correlations for aerosol mass generation rate.

Figure 12. Aerosol mass generation rate as a function of $M_s^{0.3}\phi_A^{0.36}$.

Table 1. Parameters involved in the CFD simulations.

Table 2. Showerhead physical properties, spray attributes and aerosol generation rates.